Journal of the European Ceramic Society 21 (2001) 621–632

www.elsevier.com/locate/jeurceramsoc

Effect of annealing treatments on microstructure and mechanical properties of liquid-phase-sintered silicon carbide

D. Sciti, S. Guicciardi, A. Bellosi *

CNR-IRTEC, Research Institute for Ceramics Technology, Faenza, Italy

Received 10 May 2000; received in revised form 9 August 2000; accepted 22 August 2000

Abstract

Dense hot pressed SiC based materials were produced with alumina and yttria as sintering aids in different percentages. The microstructure and mechanical properties were evaluated on as-sintered materials and related to the starting compositions. Annealing treatments were carried out at different temperatures and holding times to evaluate the possibility of a further improvement of the material properties, above all indentation toughness and high temperature properties. The attention was focused on the microstructural modifications induced by thermal treatments, i.e. formation of elongated grains, reduction and modification of secondary amorphous and crystalline phases. Mechanical properties of the annealed materials were explained on the basis of microstructural changes and compared to those of the as-sintered materials. Annealing treatments were found to be highly beneficial for improving mechanical properties and grain boundary phase microstructural changes were found to be the main factor affecting such improvements.

Keywords: Annealing; Grain boundary phase; Mechanical properties; Microstructure-final; SiC

1. Introduction

SiC ceramic is one of the promising candidate materials for high temperature structural components in heat engines, heat exchangers and wear resistant components. The most important factor that limits the applications of silicon carbide-based ceramics is their brittleness. Recently, great attention has been addressed to design starting compositions in order to favour the densification and improve fracture toughness. Silicon carbide is difficult to densify without additives, because of the covalent nature of Si–C bonding and low self-diffusion coefficient.[1] The main densification routes for silicon carbide ceramics are:- solid state sintering resulting in materials with very good properties at high temperature, but generally limited strength (<500 MPa) and toughness (2–4 MPa $m^{1/2}$); liquid phase sintering with the aid of metal oxides as Al_2O_3 and Y_2O_3 [1–9] resulting in nearly fully dense materials with very good room temperature properties but low mechanical performance at $T>1200$°C. The main limits of liquid phase sintered SiC are due to: (i) presence of amorphous or partially crystalline secondary phases, resulting from the sintering aids, which decrease high temperature fracture strength, and (ii) grain morphology which favours a relatively low fracture toughness (~3 MPa $m^{1/2}$) as cracks propagate both intergranularly and transgranularly without being appreciably deviated by the equiaxed fine microstructure.[8,9]

Recently, the possibility of an in-situ toughening of silicon carbide ceramics has been investigated by many authors,[10–25] by means of various routes, some of them based on the selection of the starting SiC powders, other based on post sintering treatments at temperatures in the range 1850–2000°C. Toughening is obtained through the development of large elongated or platelet-shaped grains that has been related to the β→α-SiC transition occurring at 1900–2000°C. Elongated grains have been shown to increase fracture toughness by crack bridging or crack deflection due to weak interface boundaries.[11–14,16,18,19] On the other hand, coarsening resulting from thermal treatment at high temperature also leads to an increase of the critical flaw which diminishes flexural strength.[10–12,19,25] Another effect due to annealing treatments is the modification of the grain

* Corresponding author.
E-mail address: bellosi@irtec1.irtec.to.cnr.it (A. Bellosi).

0955-2219/01/$ - see front matter
PII: S0955-2219(00)00254-5

boundary phase, such as its partial elimination and/or redistribution, which is due to the movement of liquid phase towards the sample surface and evaporation in the atmosphere.[15,28,29]

In this work, the microstructure and mechanical properties of liquid phase sintered SiC produced with the addition of Al_2O_3 and Y_2O_3, were studied and compared, both on as-hot pressed and on annealed materials. Because it is well known that the grain boundary phase depends on type and amount of sintering aids and governs several mechanical properties, different systems were considered, varying the total amount of additives from 6 to 10 wt.% and the Al_2O_3/Y_2O_3 ratio. In particular, annealing treatments were carried out under different processing conditions (temperature and time) in order to observe the microstructure evolution and how this change influences the mechanical properties.

2. Experimental

The starting materials used in this work were β-SiC powder (Starck BF-12, 97% β-SiC and 3% α-SiC, specific surface area: 11.6 m^2/g), β-SiC ultrafine powder (specific surface area: 42 m^2/g, synthesized through laser-induced reaction at Enea-Frascati, Italy), Al_2O_3 (Baikalox CR30) and Y_2O_3 (HC-Starck). Five different compositions were performed (see Table 1). The silica content reported in the table was determined through the chemical analysis of the oxygen of the starting SiC powders; the SAY23 mixture contains a lower amount of SiO_2 due to a thermal treatment under controlled atmosphere of the SiC Starck powder.

The powder mixes were prepared using an ultrasonic method and dried by rotary evaporator. Densification was achieved through hot pressing at 1880°C, 30 MPa, for 20–40 min. More details about processing and characteristics of the hot pressed materials are reported in previous papers.[8,9] Two sets of annealing tests were conducted in a graphite resistance furnace: the first set on $2\times2.5\times25$ mm^3 bars, cut from hot pressed discs, at 1850–1950°C for different times up to 4 h under an atmosphere of argon, in order to study microstructural evolution with annealing conditions. In the second set, hot pressed discs of the five different compositions prepared were annealed at 1900°C/3 h; afterwards samples were prepared to analyze microstructure and measure the mechanical properties. The details of the tests carried out are reported in Table 2.

The hot-pressed and annealed samples were cut, polished and plasma-etched. The microstructures were observed by SEM, and micrographs of selected samples were analysed by image analysis (Image Pro-plus 4.0, Media Cybernetics, Silver Springs, USA). The width of each grain was determined directly from the shortest grain diagonal in its two-dimensional image. The apparent length of each grain was obtained from the longest diagonal. More than 1000 grains for each specimen were used for statistical analysis. For materials with an elongated microstructure, the apparent aspect ratio obtained from two-dimensional images can underestimate the "real" aspect ratio, as statistically only 10% of the grains are cut parallel to their crystallographic *c*-axis.[30] For this reason, the R_{95} obtained from the frequency distributions, was taken to be the mean of the actual values.[11–14,23]

The mean grain size was determined through a linear-intercept method on SEM micrographs. The grain boundary phase was quantitatively estimated on digital images of the hot pressed as well as annealed samples.

Table 2
Annealing tests

Samples	Annealing cycles	*T* (C°)	Holding time (h)
I set			
SAY64, SAY23, SAY32, SAY33	3	1900	1, 2, 4
SAY64, SAY23, SAY32, SAY33	2	1850	2, 4
SAY64	1	1950	4
II set			
SAY64, SAY23, SAY32, SAY33, SSAY64	1	1900	3

Table 1
Characteristics of hot pressed and annealed (1900°C, 3 h) samples

Sample	Starting composition (%)				SiO_2 content (%)	H.P. samples density		Mean grain size (μm)	Annealed density (g/cm^3)	Weight loss (%)
	SiC[a]	SiC[b]	Al_2O_3	Y_2O_3		(g/cm^3)	(%)			
SAY64	90.0	0.0	6.0	4.0	1.49	3.24	98.8	0.54	3.21	5.5
SAY23	93.9	0.0	2.7	3.5	0.86	3.24	99.4	0.63	3.22	3.0
SAY32	94.0	0.0	3.6	2.4	1.55	3.21	98.6	0.56	3.20	4.5
SAY33	93.3	0.0	3.3	3.4	1.54	3.24	98.8	0.59	3.21	4.0
SSAY64	78.0	12.0	6.0	4.0	2.29	3.22	97.8	0.48	3.21	5.3

[a] β-SiC Starck BF-12.
[b] β-SiC ultrafine.

All samples were examined through X-ray diffraction (XRD) before and after heat treatment in order to determine SiC polytypes.

On polished surfaces, Vickers microhardness (HV) and indentation fracture toughness (K_{Ic}) were measured with loads of 9.81 and 98.1 N, respectively, using a Zwick 3212 tester. For the indentation toughness, the equation of Anstis et al. was used.[31] Young modulus (E) was measured by resonant frequency on specimens $28\times8\times0.8$ mm^3 using a H&P gain-phase analyzer. With an Instron mod 6025, flexural strength (σ), up to 1300°C, was measured on chamfered bars $2\times2.5\times25$ mm^3 (length×depth×width), in four-point bending with 20 and 10 mm as outer span and inner span, respectively, using a crosshead speed of 0.5 mm/min. For high temperature tests, a soaking time of 18 min was set to reach thermal equilibrium.

In order to evaluate the contribution of the grain boundary phase on the overall fracture toughness of the material, the percentage of transgranular fracture (PTF) along the last portion of a crack emanating from a Vickers impression corner was measured.[32]

3. Results and discussion

3.1. Microstructure of the hot pressed materials

The compositions of the starting powders and some characteristics of the hot pressed materials are shown in Table 1. The different systems were designed to evaluate sinterability and microstructural evolution in relation to amount and characteristics of liquid phase. As SiO_2 is always present on SiC powders, the characteristics of the "liquidus" and its eutectics vary according to Al_2O_3–Y_2O_3–SiO_2 phase diagrams, affecting densification and final microstructures. Compositions of SAY64 and SAY32 materials corresponded to the lowest eutectics (about 1400°C). In SAY23, the composition of additives corresponded to the stoichiometric ratio of alumina and yttria necessary to form the YAG phase ($3Y_2O_3{\cdot}5Al_2O_3$).

All samples reached densities higher than 98.5% of theoretical density. X-ray diffractograms showed that hot pressed samples contained mainly β-SiC, crystalline YAG, and traces of α-SiC 6H and 4H polytypes, already present in the starting powders; the β→α-SiC transition did not occur. The microstructure consisted of grains with a low value of aspect ratio separated by an intergranular secondary phase (examples are shown in Fig. 1a and b). In all the samples, grains were characterised by a core–shell structure typical of liquid phase sintered systems.[8,9,26,27] In fact, in the portion of the SiC grain grown on pre-existing nuclei, the presence of Al, Y and O was ascertained. YAG crystalline phase was located mainly at triple points or in randomly distributed pockets, as revealed by SEM–EDS analysis. A certain amount of amorphous silicate-like phase is supposed to have formed in all the materials owing to the reaction between the additives and the silica present in the starting powders, as already observed in literature.[4] This hypothesis is based on the following considerations: (1) The final densities of the hot pressed samples were in fact slightly inferior to the theoretical values, while no residual porosity was observed on SEM micrographs. (2) The amount of added Al_2O_3 was in

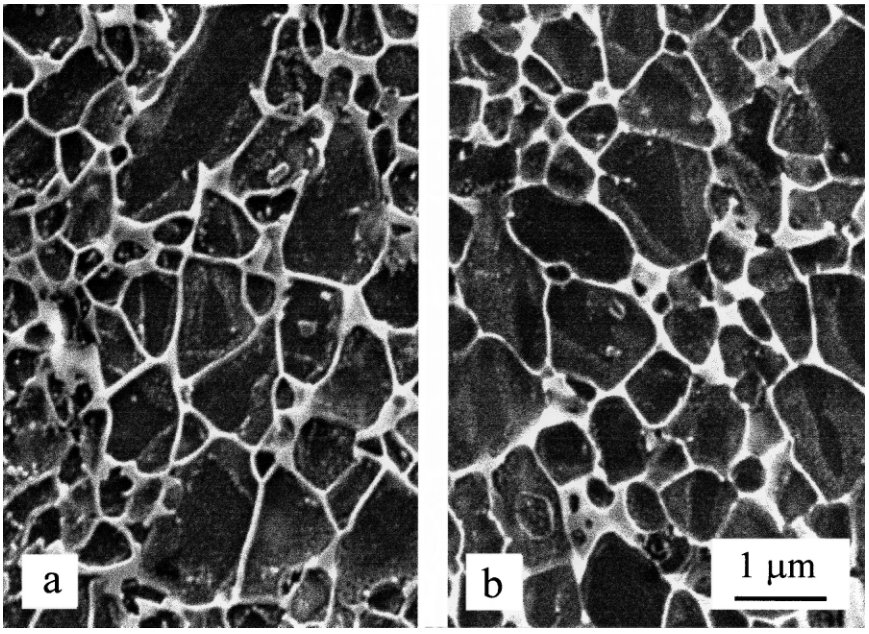

Fig. 1. Microstructural features of hot pressed samples after polishing and plasma etching: (a) SAY64, (b) SAY23.

excess in respect with the stoichiometric ratio to give crystalline YAG (apart from SAY23). This amount was considered to combine with SiO_2 to form amorphous silicate compounds in percentages from 2 to 5 wt.%, depending on the composition.

3.2. Microstructure of the annealed materials

After the annealing treatments, all the materials underwent a loss of weight. On samples heated 3 h at 1900°C weight losses ranged from ~3% (SAY23) to ~5.5% in SAY64 and SSAY64 (Table 1). Density measurements indicated a decrease of absolute density, due to the formation of volatile components as Al_2O, SiO and CO.[19] Moreover pore creation originating from microstructure rearrangement was observed in SEM micrographs. All thermal treatments gave rise to the β→α-SiC transition. In Fig. 2, X-ray diffractograms of SAY64 before and after annealing at 1900°C for 3 h show that after thermal treatments there was an evident reduction of crystalline YAG peaks, while α-SiC 6H and 4H polytypes peaks were enhanced.

Annealing treatments caused profound modifications on microstructure. The development of large elongated grains is reported in Fig. 3a and b, showing plasma etched surfaces of samples annealed 4 h at 1900°C. SiC grains underwent coarsening via both a solution-reprecipitation mechanism (with the aid of the liquid phase) and coalescence. In the former case, original β-SiC grains acted as nuclei for the growth of large and elongated grains through Ostwald ripening mechanism.[27] An example of this mechanism of regrowth is shown in Fig. 3b: the original equiaxed grain with its dark core and the first shell is surrounded by the new shell precipitated during annealing. More than one precipitated shell was often observed. Qualitative EDS analysis revealed the presence of Al and O in the lighter regions of SiC grains. It has been suggested[26,27] that the contrast gradient observed on micrographs is probably due to a different amount of oxygen and aluminium in solid solution between the external shell, the internal one and the core, which resulted in different plasma-etching rates. Coalescence contributed to grain coarsening too: in some cases elongated grains coalesced along their length resulting in a grain with lower aspect ratio; in other cases rounded grains joined in larger irregular-shaped grains. This phenomenon occurred mainly in regions poor of liquid phase and was particularly evident after long treatments or in close-to-surface areas.

Furthermore, image analysis carried out on SEM micrographs confirmed the progressive reduction of second phase amount with increasing the annealing time (as already revealed by X-ray spectra and weight losses). This is shown in the plot of Fig. 4 for SAY64 and SAY23 materials annealed at 1900°C.

In all the samples, a certain gradient in microstructural modifications was observed. The rate of grain coarsening and second phase depletion were different in the surface

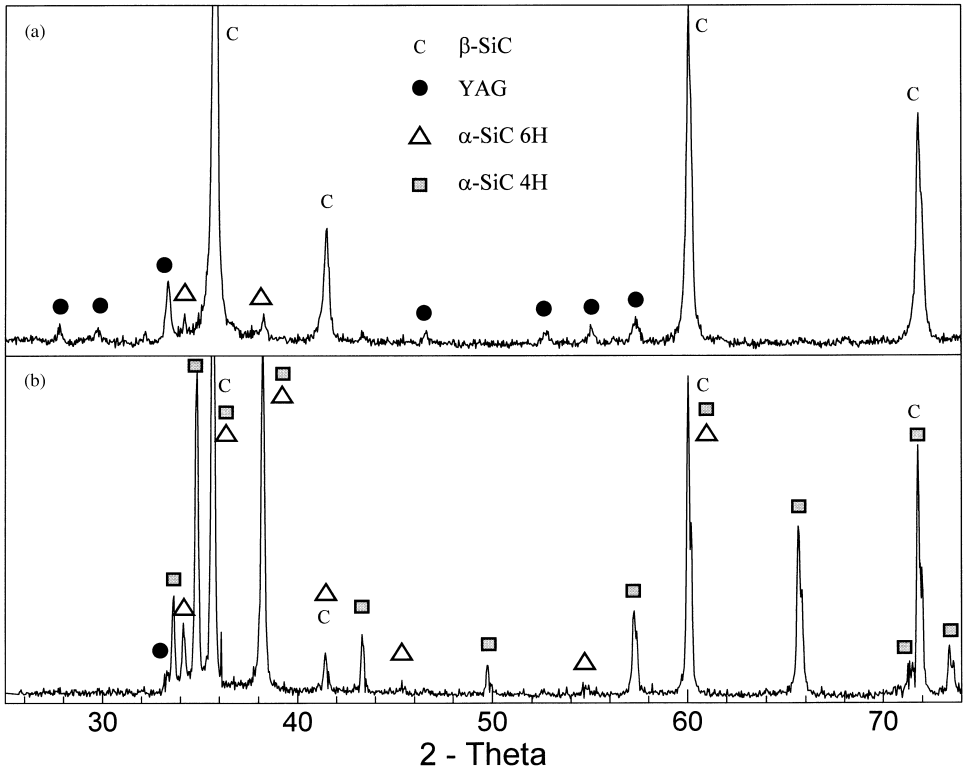

Fig. 2. X-ray diffractograms of SAY64 material (a) before and (b) after annealing treatment at 1900°C/3 h.

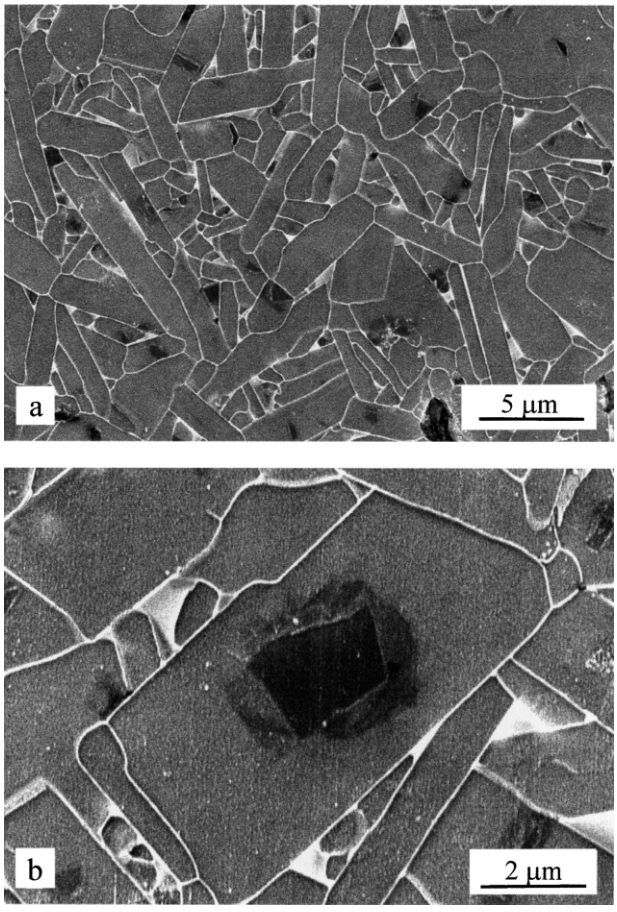

Fig. 3. Microstructural features of SAY64 samples after annealing at 1900°C/4 h: (a) plasma etched microstructure SAY64, (b) pre-existing grain with its core-shell structure and external shell grown during annealing.

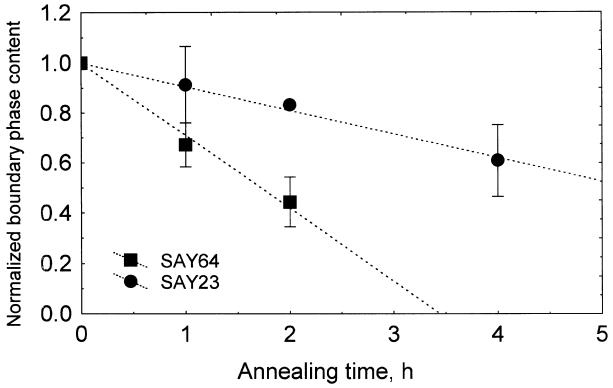

Fig. 4. Normalized grain boundary phase content as function of annealing time in SAY64 and SAY23 materials after annealing at 1900°C for 1, 2 and 4 h.

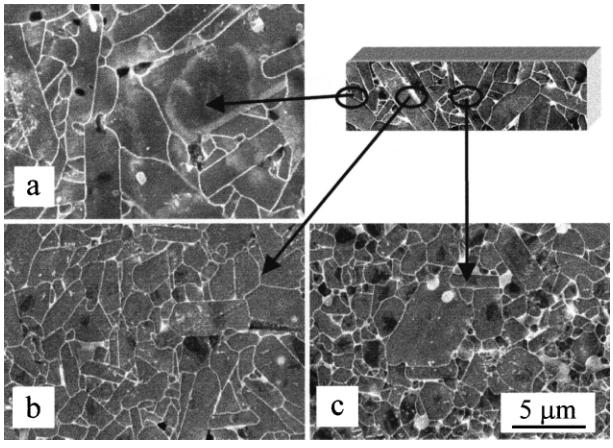

Fig. 5. Eterhogeneity in microstructural modification in SAY33 samples after annealing at 1900°C/4 h: microstructure at (a) 0.1 mm, (b) 1 mm, (c) 2 mm from the free surface.

and subsurface regions in respect with the bulk, being less pronounced with increasing distance from the surface, as shown in Fig. 5 for SAY33 annealed 4 h at 1900°C.

The main mechanism responsible for this behaviour is the movement of liquid phase towards surface and its successive volatilisation due to a carbothermal reduction: $MO(s)+C(g)\rightarrow M(g)$ or $MO(g)+CO(g)$, where M indicates the metal cation. Annealing temperatures higher than 1850°C are necessary to reach high vapour pressures of Al_2O, the most common volatile species of aluminium, while silicon monoxide has high partial pressures also in the temperature range from 1200 to 1500°C.[33] The adopted annealing conditions allow melting the silicatic and the YAG phases. Once formed, the liquid moves in the direction of low Gibbs free energy, i.e. the surface, where it volatilises as SiO or Al_2O.[28,33] When the materials were subjected to annealing, the process of carbothermal reduction of grain boundary phase was accompanied by a mass transfer through the liquid phase, which began from near-surface regions, while this was slower in the bulk. As it is generally accepted that the presence of liquid phase retards the transformation of β to α-SiC [28,29], this explains why elongated grains formed mostly on subsurface areas, sooner depleted of liquid phase, while the interior bulk retained an equiaxed morphology (although a notable reduction of second phase was observed).

In some degree, the rate of grain boundary phase removal and microstructural rearrangement was dependent on starting composition, but mostly processing parameters like annealing temperature and time showed themselves to affect the involved phenomenologies. Generally it was found that annealing treatments at $T \geqslant 1900$°C favoured the formation of elongated grains and that by increasing the holding time there was an increase of the grain size. However, although similar trends were observed for all the samples, second phase amount and composition determined some differences. The microstructural characteristics obtained through image analysis for SAY64 and SAY23 materials are shown in Table 3. In sample SAY64 in the first hour of annealing at 1900°C there was a sharp increase of the mean grain size and aspect ratio (R_{95} passed from 3.5 to

5). For longer treatments these values remained pratically constant. The frequency distribution of aspect ratios in Fig. 6a showed that there was very little variation between 1 and 4 h of thermal treatment at 1900°C. At the same time, there was a strong reduction of second phase as previously mentioned. It was estimated that after 1 h annealing, the second phase was reduced to about 65% of the initial amount (Fig. 4).

In SAY23, grain growth and formation of elongated grains were retarded in respect with SAY64 (see Fig. 7 as an example). This was related to the lower amount of liquid phase available for a solution-reprecipitation mechanism, but could also depend on a lower grade of solubility of SiC grains in a more refractory liquidus (due to the very low quantity of SiO_2 in the starting powder batch). After 1 h at 1900°C, although the mean grain size increased from 0.6 to 0.9 μm, the aspect ratio frequency distribution (Fig. 6b) did not vary significantly in respect with the as-hot pressed samples and micrographs showed that most grains still had a round shape. By contrast, for longer treatments (2–4 h), there was a gradual increase of aspect ratio and a considerable shift and broadening of the frequency distribution. Second phase reduction was somewhat slower in respect with SAY64 materials (see Fig. 4).

Comparing the values of aspect ratio, it appears that SAY23 grains were generally thicker and shorter than SAY64 grains. The lower amount of liquid phase in the SAY23 sample may have favoured the impingement and coalescence of the grains.

When the annealing temperature was raised to 1950°C, grain growth, β→α-SiC transformation and removal of grain boundary phase were further enhanced in all the materials; pores and microdefects were also originated (see Fig. 8a). On the contrary, when the annealing temperature was decreased to 1850°C, the effects on the microstructure were strongly dependent on the starting composition: also in the presence of high amounts of secondary phase (sample SAY64, Fig. 8b), the formation of elongated grains was not massive and mechanisms of partial coarsening and second phase pockets coalescence were observed. In samples with less secondary phases (i.e. SAY32, SAY33), no elongated grains were observed, but a substantial grain coalescence and rearrangement of the YAG phase in spherical particles took place. As previously mentioned, at this relatively low temperature (1850°C) the partial pressure of volatile Al_2O is too low and the carbothermal reduction

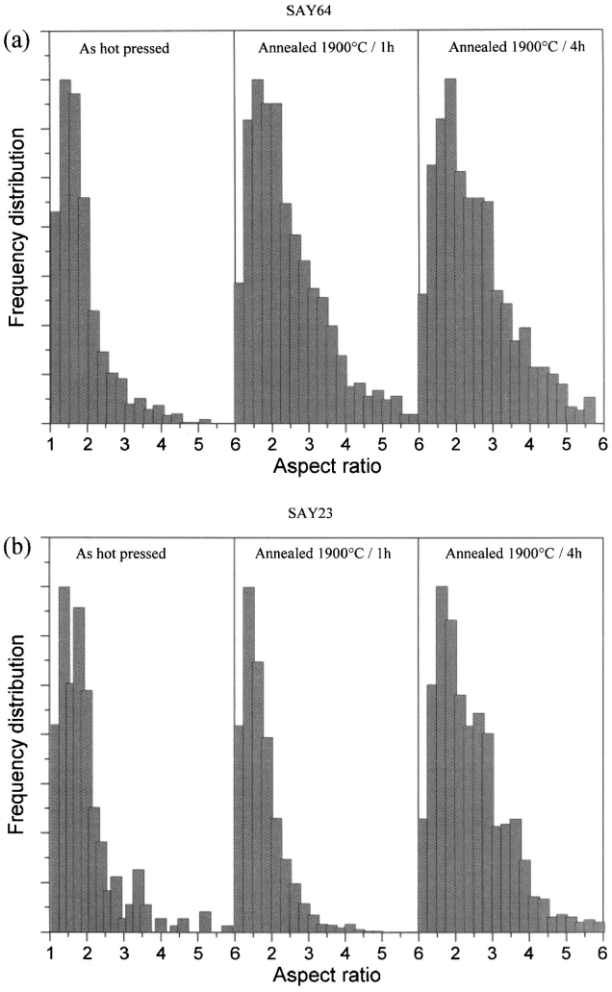

Fig. 6. Frequency distribution of aspect ratio values calculated through image analysis of as- hot pressed and annealed at 1900°C for 1–4 h. (a) SAY64, (b) SAY23.

Table 3
Indentation toughness tests on SAY64 and SAY23 samples, and related values of grain size and aspect ratio

Sample	Annealing time at 1900°C (h)	Mean grain (μm)	Grain width (μm)	Grain length (μm)	R_{95}	K_{Ic} (MPa $m^{1/2}$)
SAY64	0	0.54	0.4	0.58	3.45	3.0±0.2
	1	1.5	1.5	3.06	4.95	4.3±0.2
	2	1.6	1.7	3.58	5.05	5.5±0.2
	4	1.3	1.4	3.02	4.95	4.2±0.2
SAY23	0	0.63	0.5	0.70	3.55	3.2±0.2
	1	0.92	0.8	1.23	2.85	4.2±0.3
	2	1.62	1.5	3.04	4.18	5.2±0.4
	4	1.56	1.8	3.91	4.43	5.1±0.1

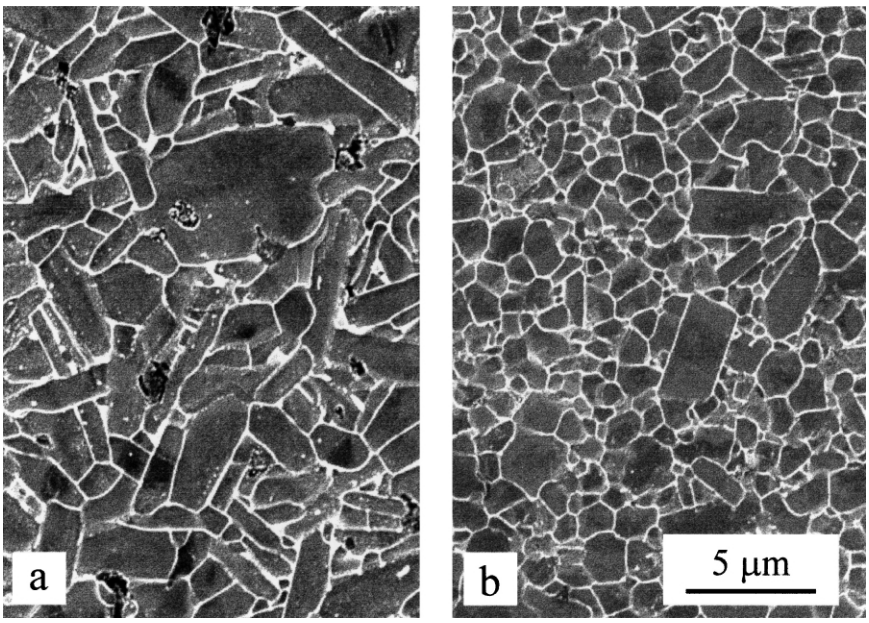

Fig. 7. Microstructural features of materials annealed 1 h at 1900°C: (a) SAY64, (b) SAY23.

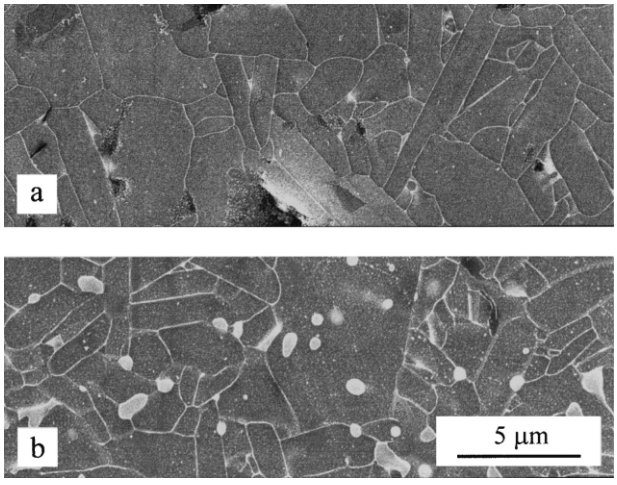

Fig. 8. Microstructural features of SAY64 annealed 4 h at (a) 1950°C and (b) 1850°C.

at the sample surface is strongly hindered. The temperature of 1850°C is therefore high enough to cause melting but not evaporation of grain boundary phase, particularly of crystalline YAG, that rearranged in spherical pockets (i.e. the shape with minimum surface energy) at triple points or inside the large grains resulting from coalescence.

From the reported results, it appeared that the best conditions to carry out annealing treatments resulting in substantial microstructural modification without creating pores and defects were a temperature of 1900°C and holding time $\geqslant 2$ h. These processing conditions were employed to treat materials for the measurement of mechanical properties which were then compared to those of the hot pressed samples.

3.3. Mechanical properties

3.3.1. Fracture toughness

The indentation fracture toughness of the hot pressed materials ranged from 2.95 to 3.17 MPa $m^{1/2}$ and should be considered statistically the same for all the materials. The fracture path was almost straight and mainly transgranular, as can be seen in Fig. 9a. After annealing, the fracture toughness increased (see Table 3). In accordance with fracture mechanics analysis,[34,35] for LPS SiC ceramics similar to those studied in this work, the fracture toughness increment was initially attributed to the increase of the aspect ratio; crack deflection and crack bridging were indicated as the toughening mechanisms.[10–12,16,18] However, the aspect ratio alone does not exhaust all the microstructural changes the material undergoes when annealed. If the grains grow equiaxially, for example, the aspect ratio remains unchanged. Moreover, the mean grain size can grow along with the aspect ratio. Bearing this in mind and considering that the toughness increment due to crack bridging should be proportional to $d^{1/2}$,[35] where d is the mean grain size, Kim et al.[13] indicated also a strong correlation between the fracture toughness of the LPS SiC materials and the square root of the mean grain size. While not wrong, the above indications invariably underestimate the contribution of the modification of grain boundary phase per se. In fact, not only do the geometrical features of the microstructure change after annealing but also the composition and crystalline state of the boundary phase. This has a very strong influence on the fracture toughness of the material as already noted by several researchers.[15,21,23,36] The results obtained in this work seem to confirm that the

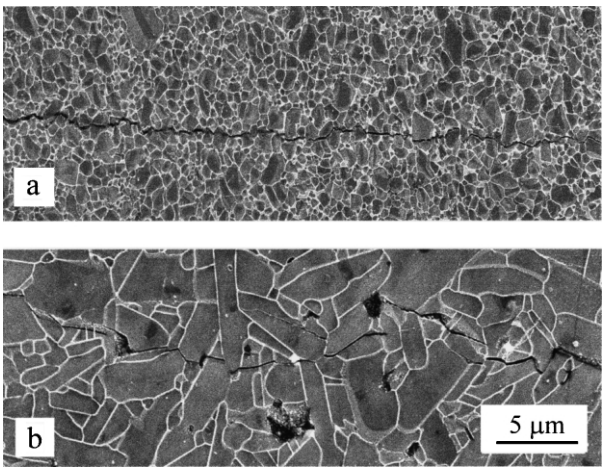

Fig. 9. SAY23 materials: crack path in (a) as-hot pressed samples, (b) after annealing at 1900°C/4 h.

modifications of the grain boundary phase are even more important than grain size/shape changes. In Fig. 10, the experimental fracture toughness values were plotted as a function of the aspect ratio (R_{95}) for the systems SAY64 and SAY23. As can be seen there are materials with almost the same aspect ratio but clearly different fracture toughness. For example, between SAY64 (1900°C, 1 h) and SAY 64 (1900°C, 2 h) the difference in fracture toughness is about a factor of 1.3. The same factor can be found between SAY23 (as-sintered) and SAY23 (1900°C, 1 h). In this case the aspect ratio (R_{95}) was even lower than that of the hot pressed one. In Fig. 11a and b experimental fracture toughness values were plotted versus the square root of the mean grain size and it can be seen that the sole mean grain size is again insufficient to explain the fracture toughness variation. Compare, for example, the annealed materials in the SAY64 system, (Fig. 11a), which have the same mean grain size but different fracture toughness. An ambiguous behaviour can be found in the SAY23 system too: compare material SAY23 (as-sintered), SAY23 (1900°C, 1 h) and SAY23 (1850°C, 4 h) where the mean grain size increases from one material to the other but the fracture toughness behaves unpredictably. To conclude, if the variation of the aspect ratio or the mean grain size are obtained by an annealing process, then it can be misleading to consider the fracture toughness directly related to morphological arrangements alone such as aspect ratio or mean grain size without considering the modifications which occur in the grain boundary phase. Considering the materials annealed at 1900°C, when the annealing time was increased from 1 h to 2 h, we found a remarkable fracture toughness increment. The crack path became more tortuous and increasingly intergranular (Fig 9b). After the annealing treatment, the grain boundary weakened and turned into preferred crack path. The fracture toughness of these materials, when compared with the as-sintered ones, showed a linear trend with the intergranular portion of the crack length (Fig. 12). The annealing

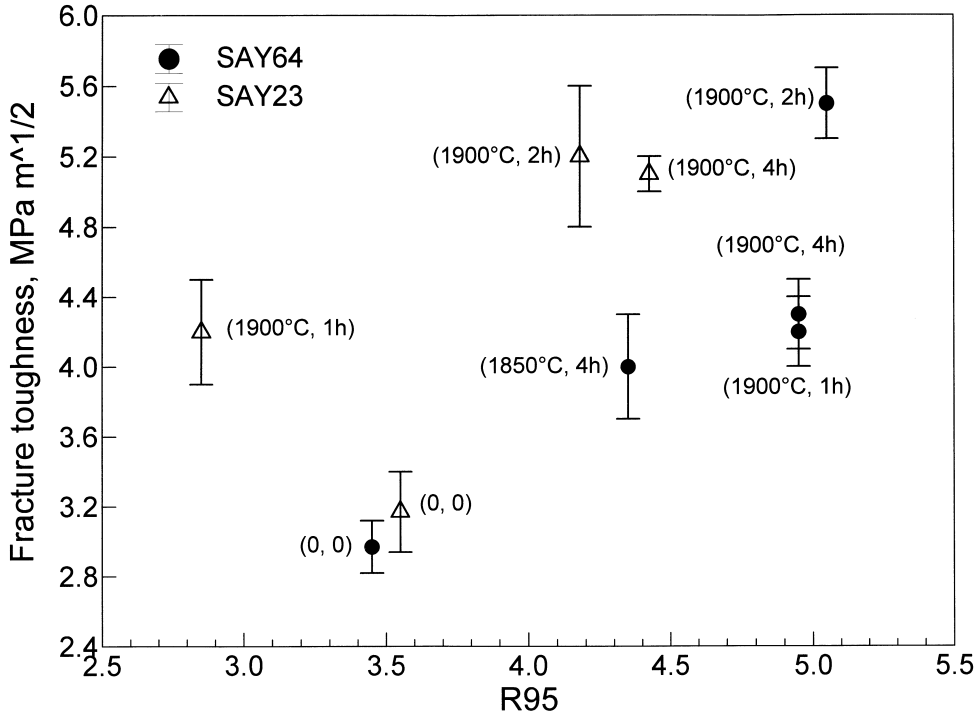

Fig. 10. Plot of fracture toughness as function of aspect ratio (R_{95}) for SAY64 and SAY23 samples. The labels of the experimental point indicate annealing temperature and holding time, respectively.

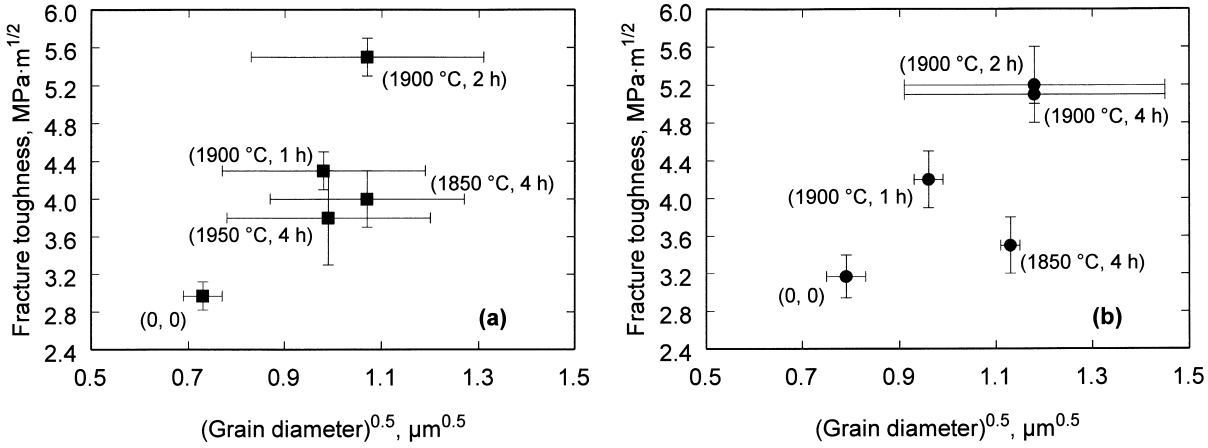

Fig. 11. Plot of fracture toughness as function of grain diameter for (a) SAY64 and (b) SAY23 samples. The labels of the experimental point indicate annealing temperature and holding time, respectively.

process induced high residual stresses from thermal expansion mismatch between SiC grains and grain boundary phase, which promoted a fracture toughness increment by residual stresses,[37] crack deflection along the grain boundaries,[38] crack bridging and induced microcracking.[39,40] Other possible toughening mechanisms such as profuse residual microcracking after annealing can be excluded as the Young's modulus of all the materials increased after a thermal treatment of 3 h. If the annealing had introduced a large number of microcracks the Young's modulus would have been reduced accordingly.[41]

Increasing both time and temperature of the annealing treatment improved the fracture toughness with respect to the as-sintered material but the increase was lower than that which can be obtained with lower annealing temperature and shorter annealing time [see in Fig. 11a material SAY64 (1950°C, 4 h)]. The process of grain boundary removal at 1950°C for 4 h has probably reached a point where the residual stresses were too high and the grain boundary fracture toughness was too-far reduced. In such kinds of anisotropic ceramics, grain boundary depletion is deleterious for the fracture toughness.[42] The materials annealed at 1850°C for 4 h, both SAY64 and SAY23, did show an improvement in fracture toughness with respect to the as-sintered materials but this improvement was lower than that obtained, for example, at 1900°C/1 h. The modification processes of the grain boundary phase did not exploit all their potential in these conditions.

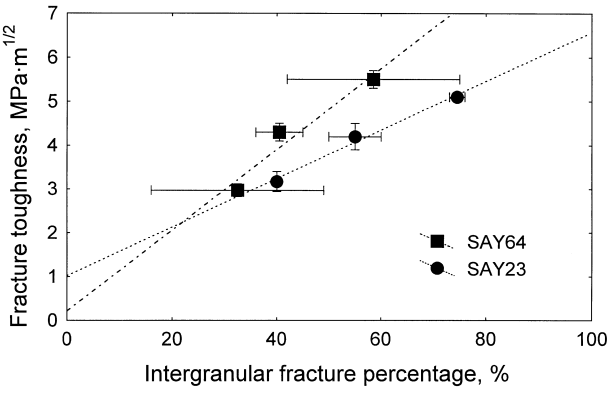

Fig. 12. Plot of mean fracture toughness vs intergranular fracture percentage in SAY64 and SAY23 materials.

3.3.2. Vicker hardness

HV values of hot pressed samples were not statistically different for the various materials investigated (Table 4)

Table 4
Mechanical properties of the hot pressed and annealed materials

Sample	HV (GPa)	Hot Pressed			E (GPa)	HV (GPa)	Annealed (1900°C/3 h)			E (GPa)
		σ (MPa)					σ (MPa)			
		RT	1000°C	1300°C			RT	1000°C	1300°C	
SAY64	22.0±0.8	746±46	528±53	159±7	386	24.1±0.9	640±17	542±47	–	412
SAY32	22.8±0.8	658±91	536±37	171±9	391	25.2±1.5	640±25	618±121	–	417
SAY33	22.3±1.5	712±105	514±66	165±31	404	24.4±1.4	571±37	618±26	–	411
SAY23	22.4±1.2	656±46	485±36	200±14	419	25.1±1.4	543±77	593±88	447±41	438
SSAY64	22.5±0.9	594±53	446±28	151	383	–	411±64	464±24	319±31	412

and similar to those found in literature.[7] After thermal treatment, a notable improvement was observed: hardness values passed from 22 to 24.5–25 GPa, statistically the same for all the materials. This result was mainly related to reduction of secondary phases which generally decrease such property.

3.3.3. Young modulus

The values of E for hot pressed samples ranged from 386 to 419 GPa being slightly inferior compared to values reported in literature (420 GPa[2]) for LPS silicon carbide (see Table 4). As the materials have the same residual porosity (< 1%) the variation observed was related to the presence of secondary phase. If, as it is supposed, amorphous silicate-like phases are present, they possess very low values of E so that even small amounts strongly affect the elastic modulus.[43] As a matter of fact, the highest value was found for SAY23 containing the lowest amount of silica and additives in the starting mixture. By contrast the lowest value was found for sample SSAY64 with the highest amount of SiO_2 and sintering aids. After annealing treatment all values were observed to increase. Again this was due to reduction or modification of the secondary phase.

3.3.4. Flexural strength

The values of σ at room temperature were observed to decrease after annealing treatment (Table 4) as reported in literature and this was directly related to grain growth associated with thermal treatment. As already found in literature,[10–12,19,25] the coarser microstructure obtained through annealing was beneficial for toughness but detrimental for flexural strength: fractography showed that typical critical defects were clusters of larger grains. This implies that there is a trade-off in simultaneously improving toughness and strength.

However, as previously seen, if the increase in toughness is related not only to grain morphology but also to second phase chemistry, a suitable choice of thermal treatment parameters that modify second phase chemistry without excessive grain growth can theoretically lead to a reinforced microstructure with little or no strength decrease.

Comparing flexural strength at 1000°C, it came out that after annealing 3 h at 1900°C there was a notable improvement for some of the samples tested (Fig. 13). Particularly for materials SAY23 and SAY33, $\sigma_{1000°C}$ was almost 20% higher than for the same materials not annealed. In the hot pressed samples, the decrease of σ with increasing temperature was due to softening of the intergranular phase:[44] its reduction after the annealing treatment (Fig. 4), resulted in the improvement observed. Good values were also maintained at 1300°C: in hot pressed samples σ decreased to 200 MPa while values as high as 450 MPa were observed, for example, in SAY23 after annealing.

4. Conclusions

Dense SiC-based materials were produced via liquid phase sintering with alumina and yttria as sintering aids. Five systems (with different amount and composition of sintering aids) were produced and the relationships between composition, microstructure and mechanical

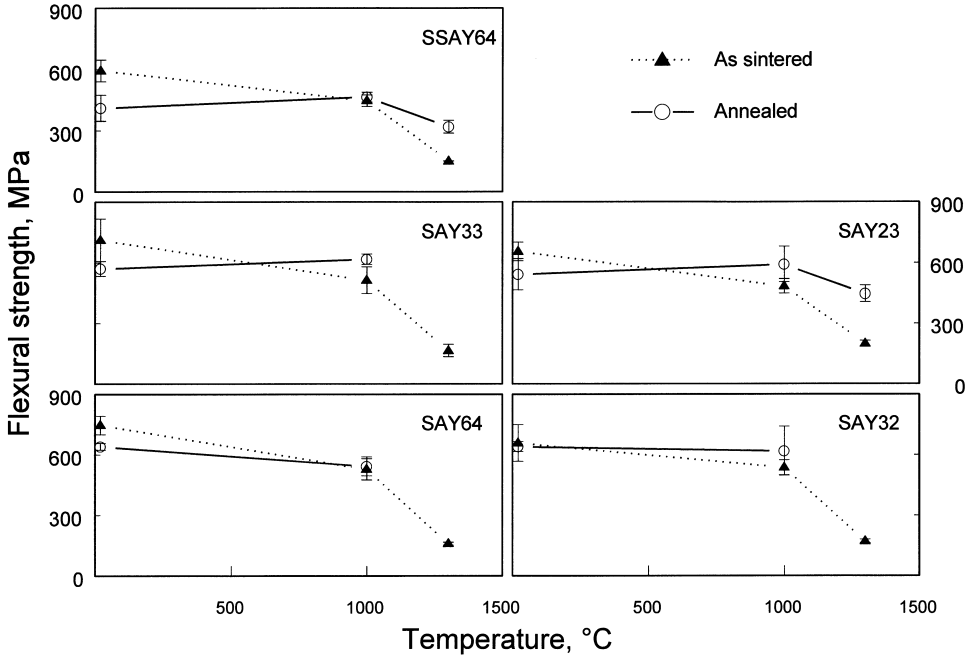

Fig. 13. Flexural strength in as-hot pressed and annealed samples as function of temperature.

properties were compared on hot pressed materials. All the systems showed a good sinterability, and the resulting materials had a fine and nearly equiaxed microstructure. Indentation toughness ranged from 2.9 to 3.2 MPa $m^{1/2}$ and the crack path was almost straight and mainly transgranular.

High strength values were obtained up to 1000°C; grain boundary phase was found to affect high temperature flexural strength as well as the Young modulus. After annealing treatments the following microstructural changes were observed:

- SiC grain coarsening (via both solution-reprecipitation mechanism and coalescence) and formation of elongated grains with gradual disappearing of the equiaxed grain microstructure.
- Reduction of secondary phase amount, through movement of the liquid phase toward surface and successive volatilization.
- Presence of a gradient in microstructural modification due to the movement of liquid phase towards the sample surface, resulting in a inhomogeneous microstructure.

It was found that the best conditions to carry out annealing treatments resulting in substantial microstructural modifications without creation of pores and defects were a temperature of 1900°C and holding time $\geqslant 2$ h.

Annealing thermal treatments on LPS silicon carbide ceramics were shown to be highly beneficial for improving the performance of these materials. Fracture toughness was found to increase with values up to 5.5 MPa $m^{1/2}$: aspect ratio and mean grain size variation are not the only factors responsible for this improvement. The presence of an intergranular phase led to thermal expansion mismatch with the matrix (SiC grains). The resulting residual stresses caused grain boundary weakening, leading to a change of the crack path from transgranular to intergranular. Crack deflection, crack bridging and induced microcracking were the main toughening mechanisms.

Vicker hardness values passed from 22 to 24.5–25 GPa and the Young modulus was highly enhanced in all the samples with values up to 430 GPa. Moreover a notable improvement was observed in flexural strength at 1000°C (almost 20% higher than not annealed samples).

Good values of RT flexural strength were maintained after thermal treatments even if slightly inferior to those of the hot pressed samples. A suitable choice of thermal treatment parameters that modify second phase chemistry without excessive grain growth may lead to an optimization of material properties with a limited strength decrease.

Compositional design and optimization of processing parameters are key factors for controlling and improving the properties of SiC-based ceramics.

References

1. Motzfeld, K., Silicon carbide: synthesis, structure and properties. In *Proceedings of the International Conference on Engineering Ceramics '92*, ed. M. Haviar. Reproprint, Bratislava, 1993, pp. 7–42.
2. Dressler, W. and Riedel, R., Progress in silicon-based non-oxide structural ceramics. *Int. J. Refractory Metals and Hard Materials*, 1997, **15**, 13–47.
3. Van Dijen, F. K. and Mayer, E., Liquid phase sintering of silicon carbide. *J. Eur. Ceram Soc.*, 1996, **16**, 413–420.
4. Falk, L. K., Microstructural development during liquid phase sintering of silicon carbide ceramics. *J. Eur. Ceram. Soc.*, 1997, **17**, 983–994.
5. Falk, L. K., Development of microstructure in liquid phase sintered SiC. In *Third Euro-Ceramics, vol. 1*, ed. P. Duran and F. Fernandez. Faenza Editrice Iberica, Spain, 1993, pp. 889–894.
6. Kleebe, H.-J., SiC and Si_3N_4 materials with improved fracture resistance. *J. Eur. Ceram Soc.*, 1992, **10**, 151–159.
7. Cutler, R. A. and Jackson, T. B., Liquid phase sintered silicon carbide. In *Ceramic Materials & Components for Engines*, 1988, pp. 309–318.
8. Bellosi, A., Sciti, D., Melandri, C. and Dalle Fabbriche, D., Liquid-phase sintered silicon carbide: processing and properties. In *Syntheses and Methodologies in Inorganic Chemistry, New Compounds and Materials*, vol. 8, ed. Litografia La Photograph (PD), 1997, pp. 269–272.
9. Sciti, D. and Bellosi, A., Effect of additives on densification, microstructure and properties of liquid- phase sintered silicon carbide. *J. Mat. Sci.*, 2000, **35**, 3849–3855.
10. Lee, S. K., Kim, Y. C. and Kim, C. H., Microstructural development and mechanical properties of pressureless-sintered SiC with plate-like grains using Al_2O_3–Y_2O_3 additives. *J. Mater. Sci.*, 1994, **29**, 5321–5326.
11. Kim, Y.-W., Mitomo, M., Emoto, H. and Lee, J-G., Effect of initial α-phase content on microstructure and mechanical properties of sintered silicon carbide. *J. Am. Ceram. Soc.*, 1998, **81**, 3136–3140.
12. Kim, Y.-W., Mitomo, M. and Cho, D.-Ho., Effect of additive amount on microstructure and mechanical properties of self-reinforced silicon carbide. *J. Mater. Sci. Lett.*, 1997, **16**, 1384–1386.
13. Kim, Y.-W., Mitomo, M. and Hirotsuru, H., Microstructural development of silicon carbide containing large seed grains. *J. Am. Ceram. Soc.*, 1997, **80**, 99–105.
14. Kim, Y.-W., Mitomo, M. and Hirotsuru, H., Grain growth and fracture toughness of fine-grained silicon carbide ceramics. *J. Am. Ceram. Soc.*, 1995, **78**, 3145–3148.
15. Hoffmann, M. J. and Nader, M., In situ toughening of non oxide ceramics — opportunities and limits. In *Engineering Ceramics '96: Higher reliability through processing*, ed. G. N. Babibi et al. Kluwer Academic Publisher, The Netherlands, 1997, pp. 133–146.
16. Padture, N. P., In situ-toughened silicon carbide. *J. Am. Ceram. Soc.*, 1994, **77**, 519–523.
17. Padture, N. P. and Lawn, B. R., Toughness properties of a silicon carbide with an in situ induced heterogeneous grain structure. *J. Am. Ceram. Soc.*, 1994, **77**, 2518–2522.
18. Cao, J. J., Moberly Chan, W. J., De Jonghe, L. C., Gilbert, C. J. and Ritchie, R. O., In situ toughened silicon carbide with Al-B-C additions. *J. Am. Ceram. Soc.*, 1996, **79**, 461–469.
19. Kim, J.-Y., Kim, Y.-W., Lee, J.-G. and Cho, K.-S., Effect of annealing on mechanical properties of self-reinforced alpha-silicon carbide. *J. Mat. Sci.*, 1999, **34**, 2325–2330.
20. Lee, J. K., Kang, H. H., Kim, Y. J., Lee, E. G. and Kim, H., Effect of YAG-phase amount on the microstructure and phase transformation during the liquid-phase sintering of β-SiC. In *Key Engineering Materials*, Vols. 161–163. Trans Tech Publ. Switzerland, 1999, pp. 263–266.

21. Mitomo, M., In-situ microstructural control in engineering ceramics. In *Key Engineering Materials*, Vols. 161–163. Trans Tech Publ. Switzerland, 1999, pp. 53–58.
22. Zhan, G.-D., Mitomo, M., Sato, H., and Kim, Y.-W., Fabrication and mechanical properties of fine grained silicon carbide ceramics. In *Key Engineering Materials*, Vols. 161–163. Trans Tech Publ. Switzerland, 1999, pp. 243–246.
23. Kim, J.-Y., Kim, Y.-W., Mitomo, M., Zhan, G.-D. and Lee, J.-G., Microstructure and mechanical properties of α-silicon carbide sintered with yttrium-aluminum garnet and silica. *J. Am. Ceram. Soc.*, 1999, **2**, 441–444.
24. Nader, M., Aldinger, F. and Hoffman, M. J., Influence of the α/β-SiC phase transformation on microstructural development and mechanical properties of liquid phase sintered silicon carbide. *J. Mat. Sci.*, 1999, **34**, 1197–1204.
25. Cho, D.-H., Kim, Y.-W. and Kim, W., Strength and fracture toughness of in situ-toughened silicon carbide. *J. Mater. Sci.*, 1997, **32**, 4777–4782.
26. Ye, H., Pujar, V. V. and Padture, N. P., Coarsening in liquid-phase-sintered α-SiC. *Acta Mater.*, 1999, **47**, 481–487.
27. Sigl, L. S. and Kleebe, H.-J., Core/rim structure of liquid-phase-sintered silicon carbide. *J. Am. Ceram. Soc.*, 1993, **76**, 773–776.
28. Lee, J.-K., Tanaka, H. and Kim, H., Movement of liquid phase and the formation of surface reaction layer on the sintering of β-SiC with an additive of yttrium aluminium garnet. *J. Mat. Sci. Lett.*, 1996, **15**, 409–411.
29. Mulla, M. A. and Krstic, V. D., Low-temperature pressureless sintering of β-Silicon carbide with aluminum oxide and yttrium oxide additions. *Am. Ceram. Soc. Bull.*, 1991, **70**, 439–443.
30. Wotting, G., Kanka, B. and Ziegler, G., Microstructural development, microstructural charcterization and relation to mechanical properties of dense silicon nitride. In *Non Oxide Technical and Engineering Ceramics*, ed. Hampshire. Elsevier, London, 1986, pp. 83–96.
31. Anstis, G. R., Chantikul, P., Lawn, B. R. and Marshall, D. B., A critical evaluation of indentation techniques for measuring fracture toughness: I, direct crack measurements. *J. Am. Ceram. Soc.*, 1981, **64**, 533–538.
32. Krell, A. and Blank, P., Inherent reinforcement of ceramic microstructures by grain boundary engineering. *J. Eur. Ceram. Soc.*, 1992, **9**, 309–322.
33. Thompson, D. P., New post-sintering treatments for improved high-temperature performance Si_3N_4-based ceramics. *Engineering Ceramics '96: Higher Reliability Through Processing,* ed. G. N. Babini et al. Kluwer Academic Publisher, The Netherlands 1997, pp. 311–326.
34. Evans, A. G., Perspective of the development of high-toughness ceramics. *J. Am. Ceram. Soc.*, 1990, **73**, 187–206.
35. Becher, P. F., Microstructure design of toughened ceramics. *J. Am. Ceram. Soc.*, 1991, **74**, 255–269.
36. Peterson, I. M. and Tien, T.-Y., Effect of the grain boundary thermal expansion coefficient on the fracture toughness of silicon nitride. *J. Am. Ceram. Soc.*, 1995, **78**, 2345–2352.
37. Shum, D. K. M., Effect of residual stresses on toughening of brittle polycrystals. *J. Mater. Sci.*, 1995, **30**, 5281–5286.
38. Pezzotti, G., On the actual contribution of crack deflection in toughening platelet-reinforced brittle-matrix composites. *Acta Metall. Mater.*, 1993, **41**, 1825–1839.
39. Claussen, N., Steeb, J. and Pabst, R. F., Effect of induced microcracking on the fracture toughness of ceramics. *Ceram. Bull.*, 1977, **56**, 559–562.
40. Ortiz, M., Microcrack coalescence and microscopic crack growth initiation in brittle solids. *Int. J. Solids Structures*, 1988, **24**, 231–250.
41. Budiansky, B. and O'Connell, R. J., Elastic moduli of a cracked solid. *Int. J. Solids Structures*, 1976, **12**, 81–97.
42. Klemm, H. and Pezzotti, G., Fracture toughness and time-dependent strength behaviour of low-doped silicon nitride for applications at 1400°C. *J. Am. Ceram. Soc.*, 1994, **77**, 553–561.
43. Kelly, A. and Macmillan, N. M., *Strong Solids*. Clavendon Press, Oxford,, 1986 p. 170.
44. Keppeler, M., Reichert, H.-G., Broadley, J. M., Thurn, G., Wiedmann, I. and Aldinger, F., High temperature mechanical behaviour of liquid phase sintered silicon carbide. *J. Eur. Ceram. Soc.*, 1998, **18**, 521–526.